Molecular Biology of the Cell
Vol. 18, 3764–3775, October 2007

GRP94 Is Essential for Mesoderm Induction and Muscle Development Because It Regulates Insulin-like Growth Factor Secretion[D] [V]

Sherry Wanderling,*†‡ Birgitte B. Simen,*†§‖ Olga Ostrovsky,†¶ Noreen T. Ahmed,¶ Shawn M. Vogen,* Tali Gidalevitz,*# and Yair Argon*§¶

*Department of Pathology and §Committee on Cell Physiology, The University of Chicago, Chicago, IL 60637; and ¶Department of Pathology and Laboratory Medicine, Children's Hospital of Philadelphia, Philadelphia, PA 19104

Submitted March 26, 2007; Revised June 18, 2007; Accepted July 6, 2007
Monitoring Editor: Jeffrey Brodsky

Because only few of its client proteins are known, the physiological roles of the endoplasmic reticulum chaperone glucose-regulated protein 94 (GRP94) are poorly understood. Using targeted disruption of the murine GRP94 gene, we show that it has essential functions in embryonic development. *grp94−/−* embryos die on day 7 of gestation, fail to develop mesoderm, primitive streak, or proamniotic cavity. *grp94−/−* ES cells grow in culture and are capable of differentiation into cells representing all three germ layers. However, these cells do not differentiate into cardiac, smooth, or skeletal muscle. Differentiation cultures of mutant ES cells are deficient in secretion of insulin-like growth factor II and their defect can be complemented with exogenous insulin-like growth factors I or II. The data identify insulin-like growth factor II as one developmentally important protein whose production depends on the activity of GRP94. Keywords: chaperone/HSP90/Insulin-like growth factors/mouse development.

INTRODUCTION

Glucose-regulated protein 94 (GRP94[1]) is an endoplasmic reticulum (ER) stress protein of the heat shock protein (HSP) 90 family. Its expression in cultured cells is modulated in response to reduced glucose level (Lee *et al.*, 1983), perturbations of calcium (Drummond *et al.*, 1987; Little and Lee, 1995) or redox potential (Kim *et al.*, 1987), inhibition of glycosylation, or activation of the unfolded protein response (Gass *et al.*, 2002). Given such variety of regulators, it is intriguing that GRP94 is absent from the yeast genome even though yeast cells respond to these stress situations much like mammalian cells. The absence from yeast indicates that GRP94 is not necessary for global protein folding in the ER, nor for the secretory process per se. Therefore, we asked what processes in multicellular organisms require GRP94.

Little is known about GRP94 expression during mammalian development, although differentiation and organogenesis present many metabolic stress conditions. GRP94 transcripts are found even in oocytes and very early embryos (McCormick and Babiarz, 1984; Kim *et al.*, 1990) and protein expression was detected in embryonic carcinoma cells, along side the expression of GRP78/BiP (Kim *et al.*, 1990), another major ER stress protein that is thought to work in concert with GRP94 (Melnick *et al.*, 1994). In 5- to 8.5-d embryos, the expression of a 100-kDa protein, which is likely but not certain to be GRP94, was highest in the embryonic and extraembryonic ectoderm and lower in the visceral endoderm. Expression was also detected in mesoderm cells emerging from the primitive streak (McCormick and Babiarz, 1984). At later stages during organogenesis (E9.5–13.5; embryonic day E0.5 is defined as noon on the day the copulation plug is found), GRP94 was expressed most obviously within the developing heart, neuroepithelium, and surface ectoderm tissues (Barnes and Smoak, 1997). These patterns of expression are likely related to energy needs in the developing embryo: GRP94 expression is highest when and where there is most demand for its function as a stress protein.

The functions of GRP94 have been explored by several genetic methods. Antisense (Li *et al.*, 1992) or ribozyme-mediated (Li *et al.*, 1991; Little and Lee, 1995) depletion of GRP94 in cultured cells have not yielded conclusive results, because they affected both GRP94 and GRP78/BiP expression. Another study depleted GRP94 levels using antisense

This article was published online ahead of print in *MBC in Press* (http://www.molbiolcell.org/cgi/doi/10.1091/mbc.E07–03–0275) on July 18, 2007.

[D] [V] The online version of this article contains supplemental material at *MBC Online* (http://www.molbiolcell.org).

† These authors contributed equally to this work and should be considered co-first authors.

Present addresses: ‡ Department of Medicine, The University of Chicago, Chicago, IL 60637; ‖ 454 Life Sciences, 20 Commercial Street, Branford, CT 06405; # Department of Biochemistry, Molecular Biology and Cell Biology, Northwestern University, Evanston, IL 60208.

Address correspondence to: Yair Argon (yargon@mail.med.upenn.edu).

Abbreviations used: AVE, anterior visceral endoderm; EB, embryoid body; ES cells, embryonic stem cells; GRP, glucose regulated protein; HSP, heat shock protein; IGF, insulin-like growth factor; VE, visceral endoderm.

[1] The official gene name, as designated in the Mouse Genome Informatics (MGI) database at the Jackson lab, is Tra1 (tumor rejection antigen 1). GRP94 is also known by the names gp96, HSP108, ERp99, and endoplasmin.

expression and showed no effect on MHC class I expression or ability to present peptides to T-cells (Lammert, 1996). Nonetheless, although induction of GRP94 and BiP by stress conditions can be inhibited by these methods, the basal expression levels remain intact and are sufficient to support cell growth. A GRP94-deficient murine pre-B lymphocyte line, 70Z/3, was isolated based on sensitivity to lipopolysaccharide (LPS) stimulation and was shown to be capable of growth in culture (Randow and Seed, 2001). A knockout *grp94 Arabidopsis* mutation shows the protein to be important for plant development (Ishiguro *et al.*, 2002). Both this *Shepherd* mutation and the 70Z/3 cell show that loss of GRP94 is not cell-lethal, but rather affects selected processes.

The above conclusion is probably related to a feature of GRP94 that distinguishes it from most other chaperones: its small number of known client proteins. In the GRP94-deficient 70Z/3 cell, surface expression of only some integrins and Toll-like receptors was affected (Randow and Seed, 2001). Similarly, we have shown that immunoglobulin biosynthesis requires GRP94 (Gidalevitz and Argon, unpublished data). It is not presently possible to predict GRP94 clients based on protein structure considerations, because there is no obvious structural element common to the known GRP94 clients. We sought to identify proteins and processes that depend on GRP94 by determining the effects of ablating GRP94 expression in the mouse.

Here we report that despite its ubiquitous expression, targeting the murine gene for GRP94 causes embryonic lethality at a specific critical developmental checkpoint: mesoderm induction. Embryonic stem (ES) cells from *grp94−/−* mice grow in culture and are capable of differentiation into multiple cell types, but not into muscle. This defect is due in part to deficient production of insulin-like growth factor (IGF)-II by the mutant ES cells, establishing IGF-II as client of GRP94.

MATERIALS AND METHODS

Cloning and Mapping of grp94 and Generation of grp94 Gene-targeted Mice

To clone and map the mouse GRP94 gene (Srivastava *et al.*, 1988), nine phages encoding overlapping portions of murine GRP94 on ~23-kb genomic DNA were isolated from a Sv129 genomic λ phage library (Stratagene, La Jolla, CA), and their *grp94* gene content was mapped by exon PCR analysis, using the porcine *grp94* gene (Dechert *et al.*, 1994) as a guide. The targeting construct was assembled in the vector pPNT1 (Tybulewicz *et al.*, 1991). An 8-kb EcoRV fragment extending from the intron between exons 3 and 4 to exon 8 was used as the right arm. The left arm was PCR-amplified and fully sequenced. It contains 1.5 kb of the gene starting in the 5′ untranslated region (UTR) and ending inside exon 3. A *Neo* gene, in the opposite transcriptional direction, separated the two arms, creating a stop in codon 62 (of the 781 codons of the mature GRP94 protein). Three vector-derived amino acids were added. Upstream of the *grp94* sequence the plasmid contained a thymidine kinase (*tk*) gene for negative selection.

Generation of grp94 Gene-targeted Mice

The targeting construct was electroporated into C1 ES cells (gift of Dr. B. Hendrikson, the University of Chicago) and clones resistant to both ganciclovir and G418 were isolated. Twelve correctly targeted clones were identified, corresponding to a ratio of 1 in 4 targeted ES clones. Six clones were expanded further, injected into blastocysts from pseudopregnant C57Bl/6 wild-type (WT) females, and implanted, and the females were allowed to produce chimeric animals. Seven male chimeric offspring with a brown coat color percentage of >75% were bred to WT C57Bl/6 females and the resulting offspring were genotyped. Heterozygotes were intercrossed to yield an F1 generation. Two independent mouse lines with germ line transmission of the disrupted gene were derived. The phenotype of both lines was indistinguishable, so the data reported here were derived from line 18, from mice backcrossed to the C57Bl/6 background for at least six generations. All procedures for breeding, maintenance, and manipulation of mice were approved by institutional animal care and use committees.

Generation of ES Cell Lines from Targeted Mice

ES cells from *grp94+/−* F4 intercrosses were isolated by flushing blastocysts from the uterine ducts of E3.5 pregnant females, as described in Hogan *et al.* (1994). One *grp94−/−* ES cell line and multiple +/+ and +/− ES lines were derived.

Immunostaining, Histology, and Whole Mount In Situ Hybridization of Embryos

Decidual swellings were dissected, fixed in 4% paraformaldehyde, embedded in paraffin, sectioned at 5–7 μm, and stained with hematoxylin and eosin (H&E). For immunohistochemistry, decidual sections were dewaxed and blocked with H_2O_2. Epitope retrieval was done with 10 mM citrate, pH 6.0. GRP94 was detected with 9G10 (Neomarkers, Fremont, CA), anti-rat IgG-biotin and then streptavidin-HRP (both Vector Laboratories, Burlingame, CA). Color detection was done with DAB (Vector Laboratories).

For whole mount in situ hybridization, embryos (E6.5 and E7.5) were dissected, fixed for 45 min in cold 4% paraformaldehyde, and processed as described (Hogan *et al.*, 1994). The embryos were hybridized at 63°C to digoxigenin-labeled probes (2 μg/ml; Roche, Indianapolis, IN). After washes at increasing stringency, probe binding was detected with Purple AP (Roche) and photographed through a dissection microscope using T-100 tungsten film (Eastman Kodak, Rochester, NY). The *brachyury* (T) template construct (a kind gift from Dr. Hermann, Max-Planck-Institut für Entwicklungsbiologie, Tübingen, Germany) was transcribed with T7 RNA polymerase (Promega, Madison, WI). All other riboprobes were synthesized using T3 RNA polymerase (Promega) from cDNAs cloned into pBluescriptIIKS+ (Stratagene).

RNA Analysis

Total RNA was isolated from entire embryos with Trizol (Sigma, St. Louis, MO). RNA was also prepared from 24-well dishes containing single embryoid bodies with the Qiagen RNeasy Mini kit (Qiagen, Chatsworth, CA). Typically, half of each RNA sample was used for cDNA preparation. Random primers (Invitrogen, Carlsbad, CA) and dNTP mixture were added, incubated for 5 min at 65°C, and rapidly cooled on ice. After addition of reaction buffer and Placental RNase inhibitor (Roche), the first strand was synthesized using either Superscript II enzyme (Invitrogen) or Sensiscript reverse transcriptase (Qiagen). RNA template was removed with RNase H (Qiagen).

PCR was performed with Elongase (Invitrogen) after standardization of samples with either HPRT or tubulin. See Supplementary Table 1 for sequences of primers and annealing conditions.

Analysis of B-cells

Splenic B-cells were purified with Lympholyte M (Accurate Chemical, Westbury, NY) according to the manufacturer's instructions. Cells were plated in triplicates in 96-well plates in the absence or presence of 5 μg LPS (*Escherichia coli* serotype 0127:B8, Sigma) per 10^6 cells in 200 μl medium and incubated for 72 h at 37°C. Supernatants were analyzed by enzyme-linked immunosorbent assay (ELISA) using an alkaline phosphatase (AP)-labeled clonotyping System (Southern Biotechnology Associates, Birmingham, AL), according to the manufacturer's directions.

Fluorescence-activated cell sorting (FACS) analysis of splenocytes was performed with fluorescent anti-IgM and anti-CD3 monoclonal antibodies (PharMingen, San Diego, CA), using standard procedures.

Differentiation Cultures of Embryoid Bodies and Analysis

ES cells were cultured by the hanging drop method at a density of 800 cells per 20-μl drop in differentiation media (ES medium without Leukemia inhibitory factor). Embryoid bodies (EBs) were cultured for 3 d in the hanging drops before transfer to the bottom of a fresh Petri dish with differentiation medium containing either 0.8% dimethyl sulfoxide (DMSO; Sigma), 10^{-8} M retinoic acid (Sigma), or no additional reagents and then grown for 5–8 more days in suspension before plating on gelatinized tissue culture dishes.

Adipocyte and neuronal cultures were grown in retinoic acid from days 3–5 or 3–11, respectively, allowed to adhere to tissue culture dishes on day 11 and analyzed on day 21 (Dani *et al.*, 1997). Adipocytes were fixed with 4% paraformaldehyde, stained with 2.5% Oil Red O (Sigma) in 2-propanol for 15 min and then washed twice each with 2-propanol water before photography.

Hepatocytes cultures grown without any additional reagents were allowed to adhere on day 5. Cells were stained with indocyanine green (ICG; Sigma) for 15 min at 37°C (Yamada *et al.*, 2002).

Muscle cell cultures were grown in DMSO. EBs were allowed to adhere on day 6 and analyzed visually for cardiac and skeletal muscle formation. When exogenous IGFs were used to complement differentiation, recombinant human IGF-I (R&D Systems, Minneapolis, MN) or IGF-II (GroPep, Adelaide, SA, Australia) were added to the cultures at day 4 at 1 μg/ml. For immunofluorescence, cells were fixed in 4% paraformaldehyde and permeabilized in 0.25% Triton X-100 for 15 min. Subsequently, the cells were stained with anti-major histocompatibility complex (MHC) mAb MF-20 (Developmental Studies Hybridoma Bank at the University of Iowa, Iowa City, IA) followed by a secondary antibody conjugated either to rhodamine or to AP (Jackson

ImmunoResearch Laboratories, West Grove, PA). The cells were counterstained with 1 ng/ml 4′,6-diamidino-2-phenylindole (DAPI) in phosphate-buffered saline, mounted, and viewed with a Zeiss Axiovert fluorescence microscope (Thornwood, NY).

For analysis of endothelial smooth muscle cells, embryoid bodies were grown in DMSO in suspension for the entire period. EBs were then fixed in 4% paraformaldehyde, double-embedded in agarose and then paraffin, and sectioned at 5 μm. They were then stained with an AP-conjugated anti-smooth muscle actin antibody (Clone 1A4, Sigma). To look for the presence of endothelial cells, sections were stained with a rabbit polyclonal αTie-2 antibody (Clone C-20; Santa Cruz Biotechnology, Santa Cruz, CA) followed by anti-rabbit IgG-biotin and streptavidin AP (both from Vector Laboratories). Color detection for AP stainings were done with Vector Red (Vector Laboratories), and slides were counterstained with Mayer's hematoxylin (Sigma) before mounting in Permount (Fisher Scientific, Pittsburgh, PA).

To examine cavity formation, sections were dewaxed, rehydrated, stained with 1% Toluidine Blue (Sigma) in 50% isopropanol, cleared with Histoclear (National Diagnostics, Atlanta, GA), and mounted in Permount.

Western Blots

Tissues were homogenized with a Dounce homogenizer, and cells and tissues were lysed in NP-40 buffer, resolved by SDS-PAGE, transferred to Hybond-C membranes (Amersham, Piscataway, NJ), and probed with the following antibodies: 9G10 (Neomarkers, Fremont, CA), anti-myogenin (Clone F5D; Santa Cruz), polyclonal anti-IGF-II (AF792; R&D), and anti-actin (AC-40; Sigma).

Quantification of IGFs

IGF-I and -II were quantified by an ELISA kit (R&D Systems), according to the manufacturer's instructions, except that color development was with 2,2'-azino-bis(3-ethylbenzthiazoline-6-sulphonic acid), and the color was measured at 415 nm. Complementation of the muscle differentiation defect was accomplished by culturing EBs in media conditioned by growth in p12 cells, which secrete IGF-I constitutively (gift of Dr. R. Baserga, Thomas Jefferson Medical School). The IGF-I level in the conditioned media was 10 ng/ml. Recombinant IGF-II was from GroPep and was used at 1 μg/ml.

RESULTS

Targeting the Murine grp94 Gene

The murine *grp94* gene, located on chromosome 10 (Maki *et al.*, 1993), was targeted in strain129 C1 ES cells (Figure 1A),

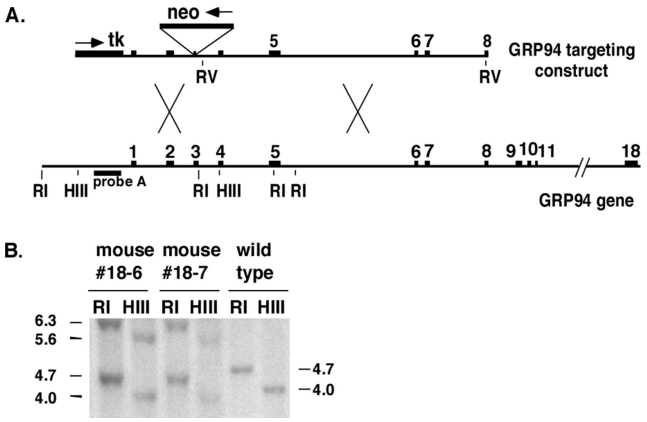

Figure 1. (A) Targeted disruption of the mouse GRP94 gene. Scheme of the murine gene and the targeting vector. The 18 exons of the GRP94 gene (black boxes) and the introns (thin lines, lengths determined by exon primer PCR and/or sequencing analysis) are drawn to scale, with a gap between exons 11 and 18. The targeting vector contains 1.2-kb 5′ homology generated by PCR amplification and 8.0-kb 3′ homology in an EcoRV fragment. The *neo* resistance cassette interrupts the coding region at the end of exon 3, 61 amino acids into the mature protein. Its transcriptional orientation is opposite that of the GRP94 gene, as marked by the arrow. The 5′ homology region is flanked by *tk*, the herpes virus thymidine kinase gene used for negative selection. (B) Correct targeting in two mice was determined by Southern blotting with probe A, located 5′ of the insertion (see arrow in A), after digestion with HindIII (H) or EcoRI (R). A new 6.8-kb EcoRI fragment and a new 6.1-kb HindIII fragment are present in the genome of the correctly targeted mice.

and six correctly targeted clones were injected into blastocysts that were implanted in pseudopregnant C57Bl/6 WT female mice. Seven males exhibiting high coat color chimerism, from two independent lines, were then bred to C57Bl/6 females, and the resulting heterozygous offspring were interbred as well as backcrossed to C57Bl/6 for 12 generations.

Southern blot analysis of genomic DNA isolated from one WT and two heterozygous F1 mice, using a probe external to the targeting construct, showed successful gene disruption (Figure 1B). RT-PCR analysis extended this finding by showing the absence of GRP94 transcripts from $-/-$ embryos (see Figure 3G). The expected protein product from the targeting construct contains 61 amino acids of the mature GRP94 protein (out of 781), plus three additional amino acids derived from the vector. This fragment is insufficient for any known activity of GRP94 such as peptide or nucleotide binding (Schulte *et al.*, 1999; Rosser and Nicchitta, 2000; Vogen *et al.*, 2002). Absence of GRP94 protein was verified by immunoblots with a polyclonal antibody (data not shown) and by immunostaining of embryonic tissues and cells with the 9G10 monoclonal anti-GRP94 (Figure 2, C and D), which recognizes an epitope within amino acids 266–347 (Robert *et al.*, 2001).

Homozygous Deletion of grp94 Has an Embryonic Lethal Phenotype

As seen in Supplementary Table 2, viable *grp94*$-/-$ mice were never obtained out of more than 900 progeny of intercrosses between heterozygotes. The fraction of heterozygous live-born mice was 55.4%, instead of the expected 66.7%. Therefore, in addition to the homozygous mutant lethality, there is slightly skewed inheritance of the knockout allele, a phenotype that is yet to be explored. To determine the stage of embryonic lethality, embryos at different stages of embryogenesis were dissected. At E14.5 and E10.5, no *grp94*$-/-$ embryos were found, and even at E8.5, only one *grp94*-deficient embryo was identified (Supplementary Table 2). Between E8.5 and E9.5, resorbing embryos were common. Between E5.5 and E7.5, however, the genotype distribution was consistent with the expected 1:2:1 Mendelian ratio. Thus, *grp94*$-/-$ embryos die around E7.5.

Up to E5.5, *grp94*$-/-$ embryos were morphologically indistinguishable from WT embryos (Figure 2, A–D). GRP94 protein expression was readily detected throughout the WT embryo (Figure 2C). A day later, E6.5, the *grp94*$-/-$ embryos were still almost indistinguishable from WT embryos (Figure 2, E–H). However, by E7.0–E7.5, a dramatic difference was observed between *grp94*$-/-$ and WT embryos (Figure 2, I and J). *grp94*$-/-$ embryos were much smaller than normal embryos and lacked any apparent lateral symmetry. Because they did not elongate properly, there was extra space in the yolk sac around the distal tip. Neither amnion nor chorion was formed, and no proamniotic cavity was evident (Figure 2J). The junction between the epiblast and the extraembryonic region was less pronounced than in WT embryos, and the endodermal cell layer appeared abnormal (Figure 2K). In normal embryos at this stage, the extraembryonic endoderm was composed of cuboidal/columnar cells with apical vacuoles, and the embryonic region of the endoderm, beyond the junction, mostly consisted of squamous cells. In contrast, the endoderm cells of *grp94*$-/-$ embryos were cuboidal in both the embryonic and the extraembryonic regions (Figure 2L, arrowheads). The parietal endoderm, attached to Reichert's membrane, was normal (Fig-

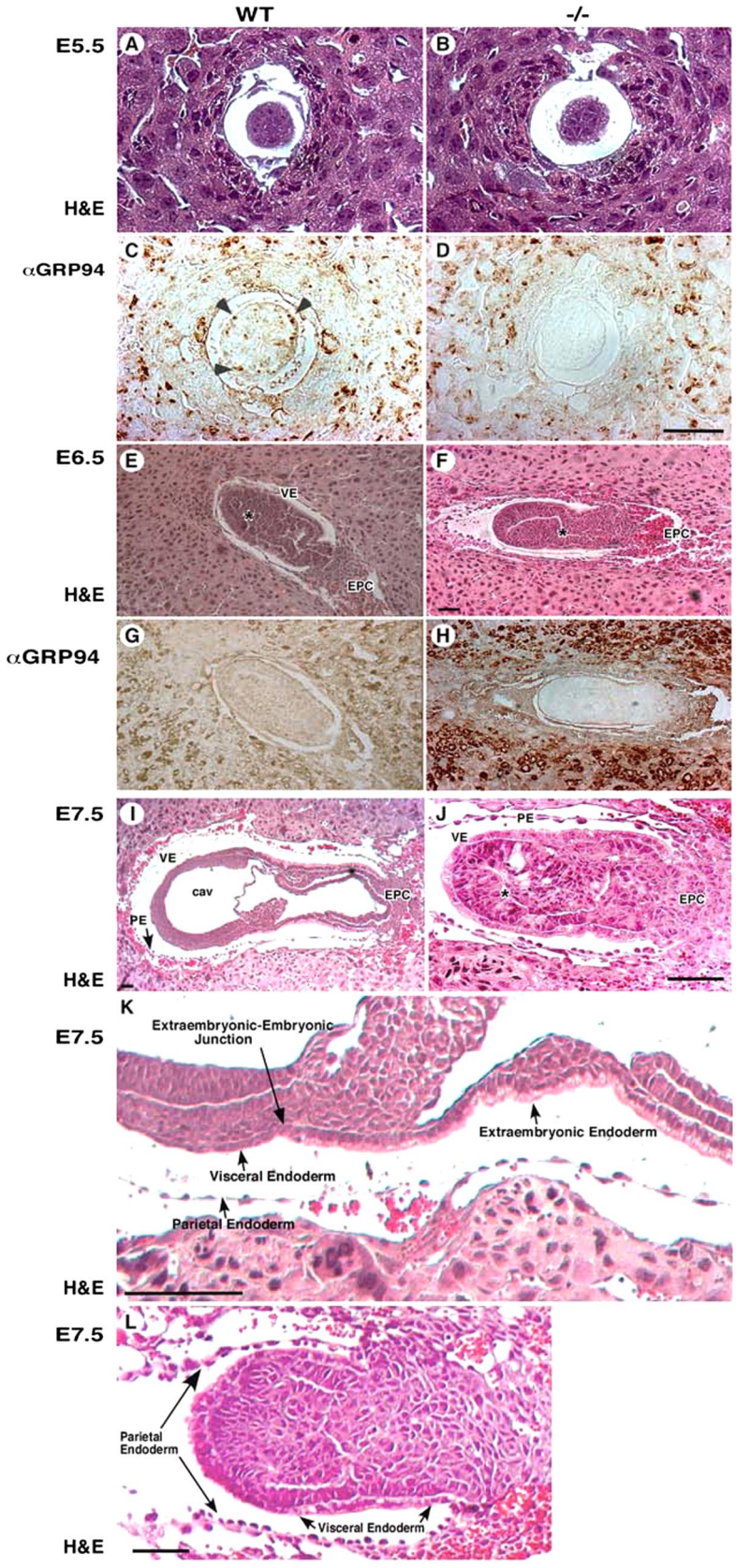

Figure 2. Grp94−/− embryos fail to gastrulate. (A–H) Histological and immunostaining analysis of WT (left) and mutant (right) embryos. Transverse sections of E5.5 embryos (A–D), E6.5 embryos (E–H), or E7.5 embryos were stained either with hematoxylin and eosin (H&E, A,B and E,F) or mAb 9G10 (αGRP94, C,D and G,H). This antibody reacts with an epitope in the second, charged domain of GRP94. Arrowheads in C denote individual cells with high GRP94 expression. VE, visceral endoderm; EPC, ectoplacental cone. (E and F) Asterisk denotes the developing proamniotic cavity. (I–L) Histological analysis of E7.5 embryos. Transverse H&E-stained sections showing the lack of mesoderm formation and lack of cavitation in −/− embryos (J; denoted with * compared with WT embryos (I). PA, proamniotic cavity; EC, exoceolomic cavity; PE, parietal endoderm. The arrows in I–L mark the junctions between the embryonic visceral endoderm and the extraembryonic visceral endoderm. (K) Higher magnification image of the embryo in I, showing the cuboidal architecture of cells on the extraembryonic side of the endoderm junction and the squamous morphology of the endoderm cells on the embryonic side of the junction. (L) A similar view of a *grp94*−/− embryo, where the VE cells on both sides of the junction are cuboidal. Note also the lack of any evidence for proamniotic cavity. The PE cells do not look different in the mutant and WT embryos. All magnification bars, 50 μm.

ure 2L, arrows). Remarkably, *grp94*−/− embryos only occasionally exhibited ingression of primitive ectodermal cells as they started to form mesoderm, and only two of the three germ layers were evident in these embryos (Figure 2, I–L).

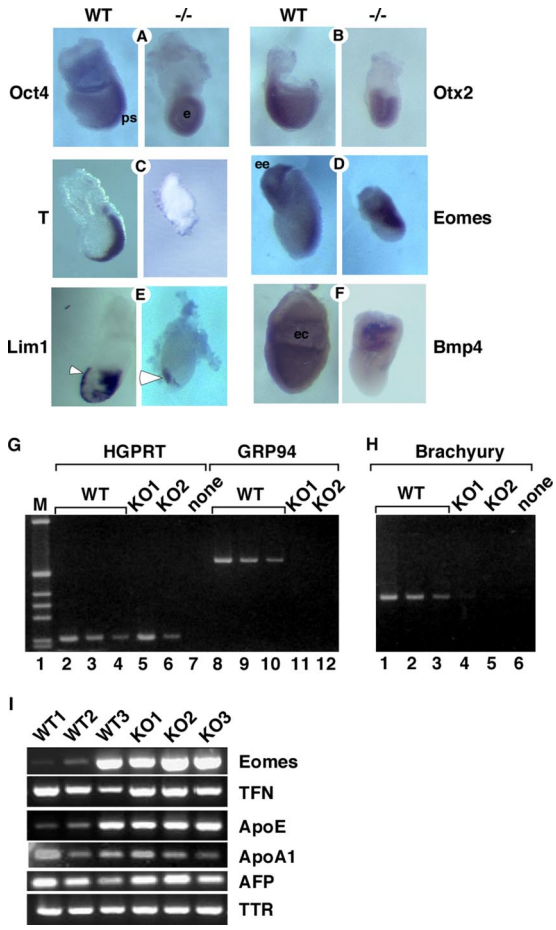

Figure 3. Grp94−/− embryos do not express mesodermal markers. (A–G) Analysis of developmental markers in g*rp94* mutant embryos by whole mount in situ hybridization. In all pairs, the WT embryo is on the left, and the mutant embryo is on the right. All embryos are E7.5 except where noted. Representative mutant and WT embryos out of 2–7 litters analyzed for each marker are shown. (A) *Oct4* is normally expressed throughout the epiblast at E6.5 and is later progressively localized to the primitive streak (ps) at E7.5 in WT embryos. Mutants show sustained overall epiblast (e) expression. (B) *Otx2* expression at E7.5 is localized to the anterior region of normal embryos, but is expressed in the entire epiblast of the mutant. (C) *Brachyury* is expressed in the primitive streak at E7.5 in normal embryos, but is not detectable in E7.5 mutant embryos. (D) *Eomes* is expressed in WT embryos in the extraembryonic ectoderm (ee) and developing primitive streak. Expression in mutant embryos at E7.5 (shown) resemble WT embryos at E6.5 (not shown). (E) *Lim1* is expressed in the AVE (arrowhead) as well as in the primitive streak and node of WT E7.5 embryos, but in mutant embryos, primitive streak expression is absent. (F) *Bmp4* expression is detected at E7.5 in the extraembryonic mesoderm lining the exocoelomic cavity (ec) of WT embryos. Mutant embryos express *Bmp4* only in the proximal extraembryonic ectoderm. (G–I) Analysis of gene expression by RT-PCR. (G) cDNA was prepared from whole E7.5 embryos carefully dissected away from maternal tissue. One wild-type (WT) and two *grp94*−/− embryos (KO1 and KO2) are shown. The amount of input cDNA was normalized using HPRT primers in the linear range of the PCR reaction (lanes 1–6). WT cDNA, at 0.25 μl (lanes 2 and 8), 0.125 μl (lanes 3 and 9), and 0.063 μl (lanes 4 and 10) are shown. Lanes 5–6, *grp94*−/− cDNA, at 11–12: 1.5 μl, from two separate −/− embryos (KO1 and KO2, respectively). The primers for GRP94 amplification span the Neo insertion site and therefore, if there is amplification of KO cDNA, the product is too large to be resolved by the gel. (H) The same cDNAs as in G were used to estimate the expression of *brachyury*, the canonical early mesoderm marker. Adjusting for the differences of input cDNA, the signal from KO1 is about four times greater than the signal from KO2, but two orders of magnitude weaker than that from WT cDNA. One of four experiments is shown. (I) RT-PCR analysis of expression of mesodermal and VE markers. cDNAs from 3 WT and 3 KO embryos were compared, normalized according to β-tubulin expression. Eomes, the T-box transcription factor eomesodermin. Its expression varies among the three WT embryos likely because WT1–3 were in decreasing age order between E6.5 and E7.5. The VE markers tested were as follows: TFN, transferrin; ApoE, apolipoprotein E; ApoA1, apolipoprotein A1; AFP, α-fetoprotein; TTR, transthyretin.

The Defect in grp94−/− Development Occurs at the Time of Gastrulation

At the time the defect in development becomes evident in the *grp94*−/− embryos, normal embryos initiate gastrulation. During this process, the visceral endoderm cells are replaced, and all three germ layers are derived from the epiblast. The visceral endoderm cells contribute only to the yolk sac and part of the extraembryonic region, but are nevertheless known to have a role in the formation of body axes (Varlet *et al.*, 1997; Dufort *et al.*, 1998). Immunochemical staining for GRP94 showed it to be expressed in all cells at either E5.5 (Figure 2C) or E6.5 (Figure 2G), but the staining was not uniform and there were clusters of visceral endoderm cells with more GRP94 than other cells (Figure 2, C and G). Importantly, the level of expression in the embryo proper and in the extraembryonic tissue was not significantly different from that in the surrounding maternal tissue.

To monitor gastrulation in *grp94*−/− embryos, we analyzed expression of transcription factors involved in cell fate specification by in situ hybridization and semiquantitative RT-PCR. Oct4, a transcription factor whose expression is detected in normal embryos already at E4.5 (Palmieri *et al.*, 1994), is expressed throughout the epiblast at E6.5 and over the next day becomes progressively concentrated in the primitive streak (Figure 3A). In E7.5 mutant embryos, the distribution of Oct4 transcripts resembles that of E6.5 WT embryos (Figure 3A). Otx2 is a homeobox transcription factor expressed ubiquitously in the embryonic ectoderm and visceral endoderm before gastrulation and is progressively restricted to the anterior region of the embryo between E6.5 and E7.5, as the primitive streak elongates (Simeone *et al.*, 1993). In E7.5 *grp94*−/− embryos, Otx2 transcripts were expressed in the entire ectoderm, similar to its distribution in WT embryos at E6.5 (Figure 3B), before the domain of expression is restricted. Both of these markers confirm at a molecular level the conclusion that *grp94*−/− embryos do not progress past the E6.5 stage.

To determine if distinct regions of the embryo were specifically affected, we tested the expression of markers for the anterior visceral endoderm (AVE). The expression of *lim-1*, which at E6.5–E7.5 is restricted to the AVE (Barnes *et al.*, 1994), is reasonably normal in mutant embryos, though the domain of expression did not extend as proximally as in WT embryos of equivalent age (Figure 3E). Similarly, a second AVE marker, *Hex* (Thomas *et al.*, 1998), is expressed in the anterior of mutant embryos (data not shown). Because a functional visceral endoderm is crucial for proper gastrulation (Duncan *et al.*, 1997), several other VE markers were tested by RT-PCR. Transcripts for transthyretin, transferrin, α-fetoprotein, and apolipoproteins A1 and E were all expressed equivalently in WT and mutant embryos (Figure 3I). In conclusion, this marker analysis indicates that at least part of the axial differentiation program, formation of the AVE organizer, is not disrupted by the deficiency in GRP94.

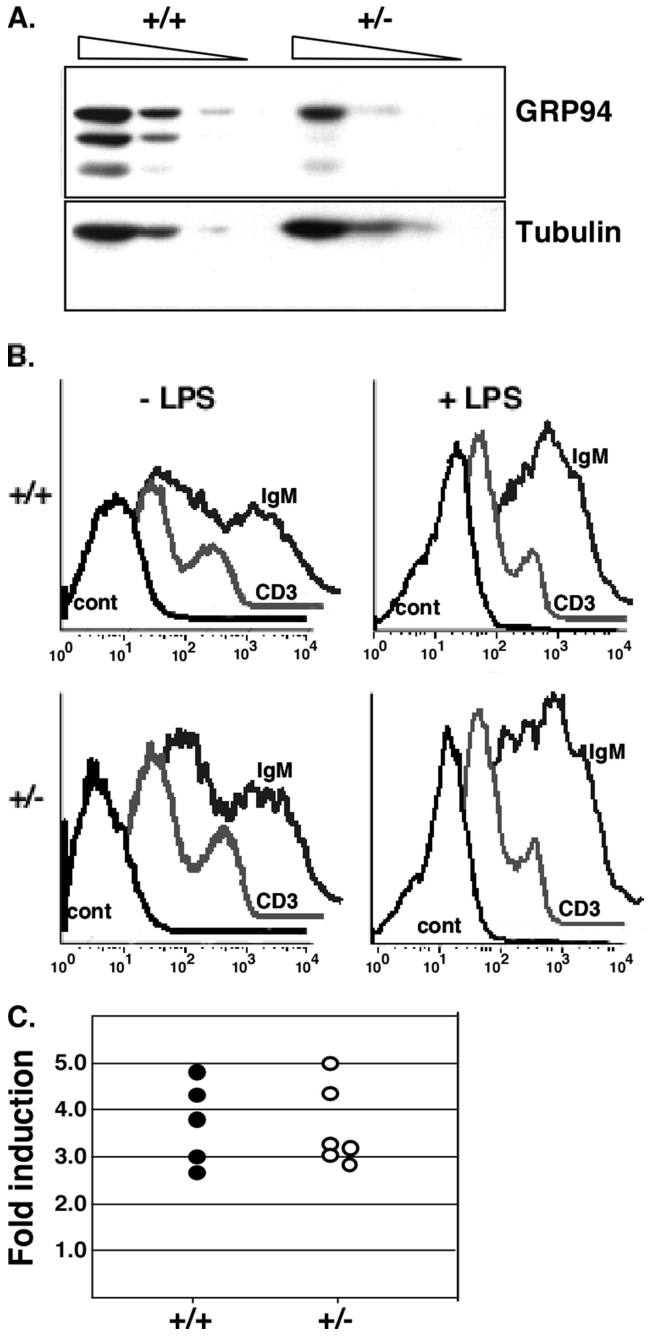

Figure 4. Heterozygous mice are normal. (A) *grp94*+/− mice have a 50% reduction in GRP94 protein. Liver homogenates were prepared from heterozygous and WT mice, and equal amounts of total protein were loaded in dilution series from left to right (100, 50, and 25 μg) and analyzed by immunoblotting with anti-GRP94 (9G10; top) or with anti-β tubulin (bottom). The three GRP94 bands are the full-length protein and two smaller degradation products (approx. 80 and 70 kDa) that are commonly seen in liver extracts. The blot shown is representative of four replicates. Essentially the same result was also obtained by immunoblots of spleen extracts (not shown). (B) Splenocyte differentiation. Spleen cells from WT (+/+) or heterozygous (+/−) mice were either cultured without treatment or treated with 50 μg/ml LPS to initiate proliferation of B-cells and differentiation into Ig-secreting cells. Three days later, the cultures were stained with anti-IgM antibodies to mark B-cells or with anti-CD3 antibodies to mark T-cells, as internal controls. Control traces, unstained cells. (C) Induction of Ig secretion in splenocytes. Spleen cells from heterozygous or WT mice where treated with 50 μg/ml LPS as above, and 3 d later the levels of Ig in the medium were determined by ELISA with either anti-μ or anti-κ antibodies. The ratio of Ig in the medium before and after LPS treatment was calculated for each spleen culture, normalized for cell number, and is plotted as the magnitude of the induction.

Another region examined was the extraembryonic ectoderm. Both normal and mutant embryos display expression of the marker *Bmp4* (Coucouvanis and Martin, 1999) in the extraembryonic ectoderm at E7.5 (Figure 3F), but in *grp94*−/− embryos the expression domain of *Bmp4* is restricted to the proximal extraembryonic ectoderm, whereas in WT embryos it extends also to the extraembryonic mesoderm lining the exocoelomic cavity (Figure 3F). This is again consistent with arrested differentiation at E6.5 without an obvious effect on the extraembryonic ectoderm.

Analysis of three markers shows that *grp94*−/− embryos are deficient in mesoderm induction. The expression of *brachyury* (T), an early mesoderm marker (Wilkinson *et al.*, 1990), could not be detected in E7.5 *grp94*−/− embryos by in situ hybridization, whereas in the normal littermates *brachyury* was expressed in the primitive streak (Figure 3C). Absence of or very low expression of *brachyury* was confirmed by RT-PCR amplification of transcripts from individual E7.5 embryos with *brachyury*-specific primers (Figure 3H). A later mesoderm marker, *pMesogenin1* (Yoon *et al.*, 2000), was also undetectable by RT-PCR in mutant embryos (data not shown, N = 2). Another T-box transcription factor, Eomes, which is involved in gastrulation and mesoderm induction at an earlier stage than *brachyury* (Russ *et al.*, 2000), was expressed in −/− embryos. By whole mount in situ hybridization, *eomes* was expressed in WT E7.5 embryos primarily at the primitive streak and in the extraembryonic region (Figure 3D). In *grp94*−/− embryos, the expression domain of *eomes* comprised a larger portion of the egg cylinder, including the area where the primitive streak would be expected to develop (Figure 3D). The *eomes* expression pattern in E7.5 *grp94*−/− embryos was very similar to that of E6.5 WT embryos (Ciruna and Rossant, 1999). Consistent with this result, PCR analysis showed that *eomes* transcripts are readily detected in mutant embryos at a level intermediate within the range seen in WT E7.5 embryos (Figure 3I). The variability in *eomes* PCR amplification from individual WT embryos reflects the progressively restricted expression of *eomes* between E6.5 and E7.5 (Ciruna and Rossant, 1999); evidently, some of the dissected embryos were older than the others. Together, the RT-PCR, hybridization analysis, and morphological data indicate that the defect in *grp94*−/− development is at an early gastrulation stage when the primitive streak should develop. Furthermore, GRP94 activity appears to be needed between the initial wave of *eomes* expression and the normal time of *brachyury* expression.

Live-born Heterozygotes Are Normal

No phenotypic differences were observed between live-born heterozygote and WT mice. Appearance, weight, life span, and fertility were all normal (data not shown). To investigate whether GRP94 expression from the remaining allele was up-regulated, protein expression in livers and spleens of *grp94*+/+ and +/− mice was quantified by immunoblotting. The amount of GRP94 in heterozygous tissues was approximately half of WT levels (Figure 4A), indicating that there was no up-regulation of expression from the WT allele. Furthermore, the levels of three other major ER chaperones,

BiP, calnexin, and ERp72, were identical in heterozygotes and WT animals (Gidalevitz and Argon, unpublished data). Thus, the decreased expression of GRP94 was not compensated for by up-regulation of these ER chaperones, and half the normal level is sufficient for mouse development.

Because GRP94 is up-regulated during the differentiation of resting B lymphocytes into plasma cells (Lewis *et al.*, 1985; Wiest *et al.*, 1990), we examined the effect of having only half as much GRP94 on B-cell differentiation and on immunoglobulin secretion. Numbers of both T- and B-cells were similar in +/− and +/+ mice. Spleen cells were examined by FACS for surface immunoglobulin (Ig) expression and by ELISA for Ig secretion, before and after stimulation with LPS. As seen in Figure 4B, there was no difference in the level of surface Ig expression either before or after 3 d of ex vivo LPS stimulation. Third, no significant difference was detected in the level of IgM secreted by *grp94*+/− and +/+ splenocytes (Figure 4C). Therefore, half the normal level of GRP94 is sufficient to support Ig secretion, a process that entails physiological ER stress response (Lewis *et al.*, 1985; Wiest *et al.*, 1990).

Mutant ES Cells Can Differentiate in Culture

To investigate the differentiation potential of *grp94*-deficient ES cells, a matching set of −/−, +/−, and +/+ ES cells were derived from a single litter of E3.5 blastocysts. EBs from these cells were cultured in medium containing either 0.8% DMSO, 10^{-8} M retinoic acid, or no additional reagents, and after 6–11 d in suspension, cultures were allowed to adhere to gelatin-coated plates. Within the next 9 d, distinct cell types became evident in these cultures. In retinoic acid–treated cultures, neuron-like cells developed from *grp94*−/− cells at times and frequencies similar to those observed in cultures of GRP94-containing ES cells (Figure 5A and B; Bain *et al.*, 1995). Similarly, indocyanine green–positive, hepatocyte-like cells were abundantly present in differentiation cultures (Figure 5, C and D; differentiation as in Yamada *et al.*, 2002). Thus, −/− ES cells can give rise to both ectoderm- and endoderm-derived cells. Remarkably, despite the failure to develop mesoderm in the embryos, *grp94*−/− ES cells did give rise to oil red O–positive adipocyte-like cells, which are of mesodermal lineage (Dani *et al.*, 1997; Figure 5, E and F). The frequency of adipocyte differentiation was in fact higher in cultures of −/− cells than +/+ or +/− cells. There was also no deficiency in differentiation of endothelial cells (Figure 5, I and J). Thus, the absence of GRP94 does not per se preclude the ability to differentiate into cells of all three germ layers, including mesodermal differentiation.

When EBs were grown in suspension cultures, both WT and −/− EBs formed well-defined spherical EBs after 9 d, though like the embryos, −/− EBs are smaller than WT EBs (Figure 5, G and H). In contrast to the inability of *grp94*−/− embryos to cavitate properly (Figure 2J), −/− EBs do form a central cavity. However, the organization of the peripheral cell layers is abnormal in −/− EBs, and after prolonged growth in suspension they have fewer types of differentiated cells (data not shown).

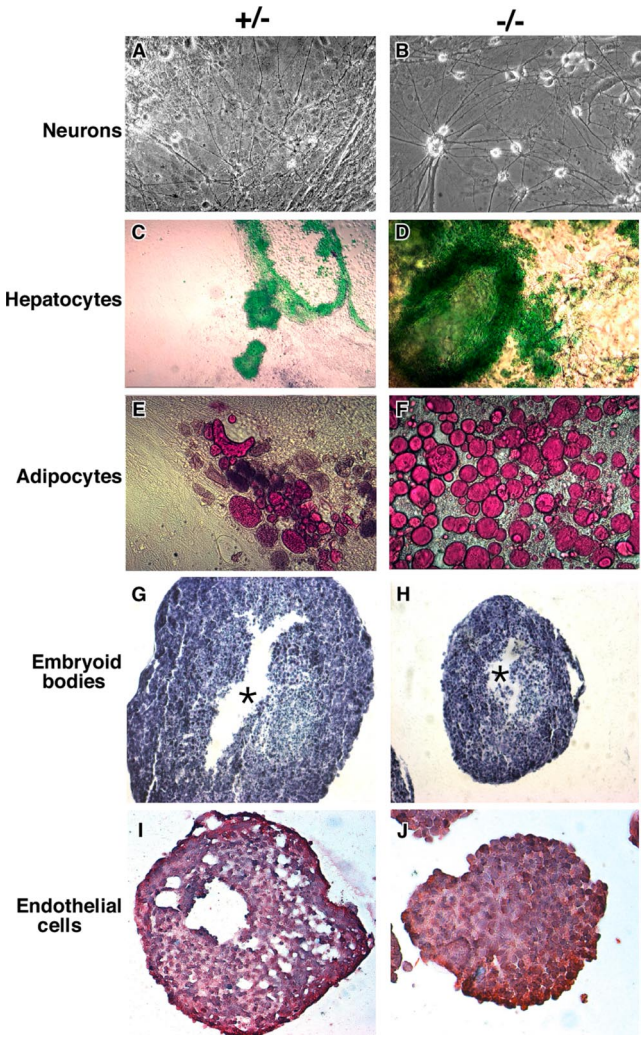

Figure 5. Differentiation potential of *grp94*−/− ES cells. *grp94* heterozygous (+/−) ES cells (A, C, and E) and *grp94*-deficient (−/−) ES cells (B, D, and F) were aggregated into embryoid bodies and induced to differentiate. (A and B) Differentiation into neurons (ectodermal lineage) in the presence of retinoic acid. Note the neuronal-like cells in both cultures. (C and D) Differentiation for 5 d without additives. Cultures were stained with indocyanine green to mark hepatocytes (endodermal lineage). (E and F) Differentiation into adipocytes (mesodermal lineage) in the presence of retinoic acid. Note the red cells that have taken up Oil red O, a characteristic of adipocytes. (G and H) Cavity formation in EBs. EBs were cultured in hanging drops for 9 d, fixed, sectioned, and stained with toluidine blue. Asterisks, the central cavity that forms in both the +/− and −/− EBs. Both panels were photographed at the same magnification. (I and J) Differentiation of endothelial cells. EBs were cultured in hanging drops for 9 d with 0.8% DMSO, fixed, sectioned, and stained with monoclonal anti-Tie-2 (red cells), and counterstained with hemotoxylin (blue-purple).

Mutant ES Cells Fail To Differentiate into Muscle

In contrast to the above differentiation results, *grp94*−/− ES cells did not give rise to muscle lineages. DMSO-treated *grp94*+/+ or +/− cells developed mounds of rhythmically contracting cardiomyocyte-like cells after day 9 of culture (Boheler *et al.*, 2002; Supplementary Video in Supplementary Figure 1). Although cardiomyocyte differentiation was consistently observed in differentiation cultures derived independently from more than 120 GRP94-containing embryoid bodies, it was never observed in parallel cultures from *grp94*−/− EBs. Furthermore, −/− cells did not give rise to skeletal myotubes, elongated, multinucleated cells that stained positively for myosin heavy chain (compare Figure 6A with 6B). This phenotype was verified biochemically: proteins from individual embryoid bodies were separated by SDS-PAGE and analyzed by immunoblotting. Cultures of C2C12 cells that had been induced to differentiate (Yaffe and Saxel, 1977) served as positive controls. Mutant EBs ex-

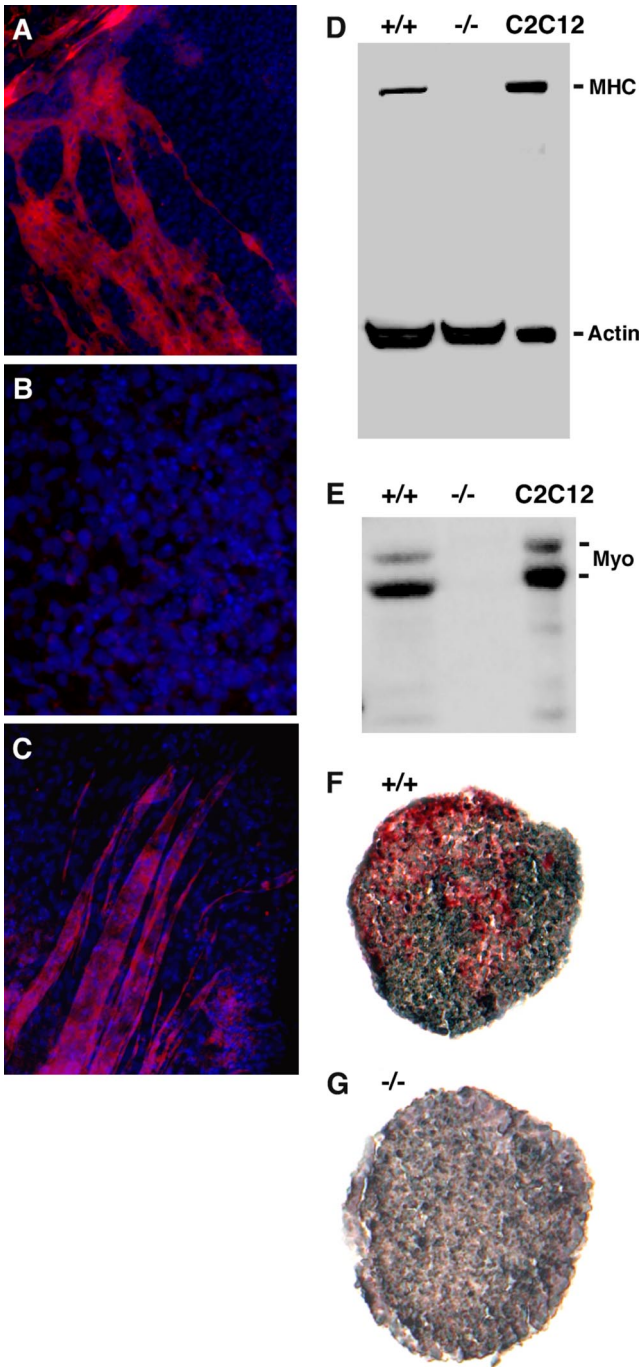

Figure 6. Mutant ES cells fail to differentiate into skeletal muscle. (A) Immunofluorescence of a culture of WT ES cells induced to differentiate into muscle. Cells were fixed and stained with anti-myosin heavy chain antibody MF20 and counterstained with DAPI to highlight nuclei. Note the characteristically shaped myotubes that are positive for myosin heavy chain. (B) A similar immunofluorescence staining of a differentiation culture of mutant ES cells. (C) A subclone of the mutant ES cells (14.1.13) that express GRP94 at levels comparable to WT levels was tested in the differentiation cultures described above. After 19–25 d the cells were stained with anti-myosin as in A. Shown is a field of clone 13 cells. Similar results were obtained with clone 14.1.2. (D) Immunoblot analysis for expression of myosin heavy chain (MHC) in lysates of wild type (+/+) and mutant (−/−) embryoid bodies and in a lysate of C2C12 cells (American Type Culture Collection, Manassas, VA) that were induced to differentiate by serum withdrawal for 48 h. The anti-actin used as a loading control recognizes nonmuscle actin as well as muscle actin. (E) The same membrane shown in C was reprobed for expression of the transcription factor myogenin. (F and G) Cultured EBs were fixed after 9 d and sectioned. Immunohistochemistry was performed with AP-labeled monoclonal anti-smooth muscle actin antibody (red), and sections were counterstained with hematoxylin (purple). WT EBs (F) were positive for smooth muscle actin, but KO EBs (G) were negative.

pressed no detectable myosin heavy chain (Figure 6D). They also expressed no detectable myogenin, a transcription factor characteristic of muscle cell differentiation (Figure 6E; Myer *et al.*, 2001). The differentiation defect extended also to smooth muscle, as indicated by the failure to detect expression of smooth muscle actin in EBs that differentiated in suspension cultures (Figure 6, F and G).

To verify that these deficiencies are due to the missing activity of GRP94, two −/− cell lines re-expressing GRP94 were independently derived. Both clones were able to fuse in culture into myotube-like multinucleated cells that were myosin heavy chain-positive (Figure 6C), showing that the muscle differentiation defect is due, at least in part, to the absence of active GRP94 and not to a secondary adaptation of the −/− cells. We conclude that the ablation of *grp94* specifically impairs the capacity of ES cells to differentiate into muscle lineages.

Mutant Embryoid Bodies Are Deficient in IGF-II Production

Muscle development is known to be regulated by IGFs, and during early embryogenesis the relevant one is IGF-II (Baker *et al.*, 1993). We therefore examined IGF-II expression in WT and *grp94*−/− ES cells and EBs. Semiquantitative immunoblots of whole cell lysates show that although proIGF-II is undetectable in undifferentiated ES cells of either genotype, it could be detected in lysates of individual WT EBs (Figure 7A). EBs with contractile mounds of cells contained higher levels of pro-IGF-II compared with EBs that did not contract (Figure 7A). *grp94*−/− EBs contained much reduced levels of pro-IGF-II (Figure 7A). The difference was confirmed by quantitation of IGF-II secretion by ELISA: *grp94*−/− EBs secreted barely detectable levels of IGF-II compared with WT EBs (Figure 7B).

When *grp94*−/− EBs were cultured in the presence of exogenous IGF, the muscle differentiation defect was partially complemented. Although we have not yet been able to restore contractility to the cultures, when supplemented with IGF *grp94*−/− cells were able to differentiate and fuse into myotube-like syncitia with 2–4 nuclei (Figure 7, C–E), which expressed myosin heavy chain (Figure 7, F–H). Either IGF-I or IGF-II was effective in this complementation, consistent with the ability of either IGF to signal via the same IGF1 receptor (LeRoith and Roberts, 2003). Both the responsiveness to exogenous IGF and staining with anti-IGF1R (data not shown) demonstrate that receptor expression is intact in *grp94*−/− EBs. We conclude that the dependence of muscle development on GRP94 is due to failure to secrete sufficient amounts of IGF-II in the absence of the active chaperone.

DISCUSSION

Given the abundant and ubiquitous expression of the chaperone GRP94, the phenotype of its targeted disruption is rather surprising in its specificity. The embryonic lethality shows that *grp94* is an essential gene for mouse development because it is needed for mesoderm induction. Furthermore,

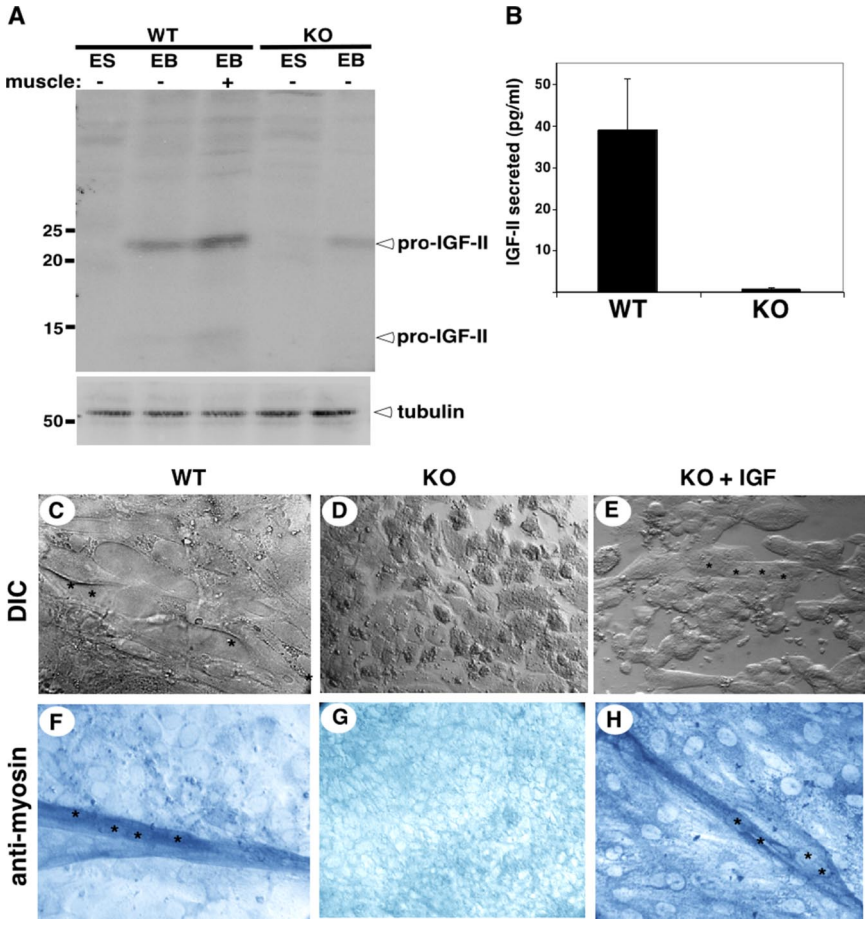

Figure 7. IGF defect and its complementation. (A) Immunoblots of IGF-II in wild-type (WT) and mutant (KO) embryoid bodies. Embryoid bodies (EB) from each genotype were cultured for up to 25 d under conditions promoting muscle differentiation. Single EBs that either displayed contractile behavior (+ muscle) or did not contract (− muscle) were lysed, and their proteins were resolved by SDS-PAGE and probed with anti-IGF-II. The band at 22 kDa is the unprocessed prohormone, and the band at 14 kDa is the result of the first of two proteolytic cleavages (Duguay, 1998). Bottom panel, immunoblot with anti-tubulin, used a loading control. (B) ELISA of IGF-II secreted by WT and KO embryoid bodies. The average ± SD of IGF-II secreted by individual embryoid bodies per milliliter of culture in a 24-h period is plotted for each geneotype. n = 3. (C–E) Myoblast fusion in cultured EBs. ES cells of either WT or KO genotype were cultured under conditions that give rise to extensive myoblast fusion in WT cells (C). Asterisks highlight individual nuclei under DIC optics. (D) KO ES cells under the same conditions remain as individual, separate cells. (E) KO ES cells supplemented with recombinant IGF-I display multiple cyncitia, each with 2–4 nuclei, as indicated by asterisks. Similar results were obtained by adding exogenous IGF-II. All cultures were photographed at the same magnification. (F–H) Myosin expression in cultured EBs. Cultures as in C–E were stained with anti-myosin heavy chain, followed by AP-conjugated secondary antibody.

GRP94 is essential for embryoid body differentiation into muscle because it regulates the secretion of IGF.

Although GRP94 is expressed in early postimplantation embryos (Li and Lee, 1991 and this work), the first developmental stage that critically depends on GRP94 is gastrulation and mesoderm induction, around E6.5. In the absence of GRP94, development is arrested at this stage and the major developmental defects are failure of primitive streak formation or induction of mesoderm. Analysis of transcripts of several mesoderm markers suggests that the differentiation program is blocked between the expression of *eomes* and *brachyury*. The failure to induce mesoderm differentiation, a process that specifies cell fate through interactions with other cells, is consistent with the molecular role of an ER chaperone like GRP94.

GRP94 is required during development earlier than HSP90β, a related cytosolic chaperone, whose ablation arrests mouse development at E9.0-E9.5 due to defective placental development (Voss *et al.*, 2000). The requirement for GRP94 is also earlier than for calreticulin, another Ca^{2+}-binding ER chaperone, whose ablation arrests development around E9.0 because of defective cardiac development (Guo *et al.*, 2002). These differences presumably reflect distinct client proteins that depend on each chaperone for proper expression. The developmental arrest of *grp94−/−* embryos is not due to dilution of maternally inherited protein and is likely autonomous to the embryo. Importantly, GRP94-deficient cells are capable of proliferation and even differentiation in culture, showing that GRP94 is not essential for these processes. This conclusion extends the observations of Randow and Seed (2001), who showed that GRP94 is not essential for growth and proliferation of a pre-B-cell line, and of Ishiguro *et al.* (2002), who showed that a naturally occurring *Arabidopsis* GRP94-deficient mutant is arrested in development. Therefore, we infer from the precise stage of developmental arrest that GRP94's activity is necessary for proper execution of an important checkpoint.

A developmental defect is also manifest in the phenotype of *grp94−/−* ES cells in culture. These cells are capable of differentiation into multiple lineages derived from all three germ layers, showing that there is no global inability to differentiate. Rather, GRP94 is required for specific lineage decisions, because mutant ES cells fail to give rise to cardiac, skeletal, or smooth muscle cells, which are all mesoderm-derived. Like mesoderm induction in the primitive streak of the embryo, differentiation of muscle cells in culture depends on signaling by extracellular factors, such as the IGFs (Lee *et al.*, 1990; Dupont and Holzenberger, 2003), to initiate specific gene expression programs. Indeed, we find that *grp94−/−* cells are deficient in IGF-II production (Ostrovsky and Argon, unpublished data), a major mitogenic factor in early mouse development expressed in several types of cells (DeChiara *et al.*, 1990; Baker *et al.*, 1993; Liu *et al.*, 1993). That this defect is a primary consequence of the absence of GRP94 is shown by the ability of exogenous IGF to partially rescue the muscle differentiation defect of *grp94−/−* cells. IGF-I and IGF-II share the same IGF1R receptor (Baker *et al.*, 1993), and IGF-I can substitute for IGF-II in a number of cells and tissues (Dupont and Holzenberger, 2003). When supplemented with either IGF, the ability of *grp94−/−* cells to fuse

into multinucleated myotube-like cells that express myosin heavy chain is restored. These cells are still not able to differentiate further into contractile myotubes, evidently because another, yet unknown factor is still missing in the absence of GRP94. Nonetheless, the ability to restore part of muscle differentiation points to IGF-II as a developmentally relevant target protein that depends on GRP94 activity for its secretion. As shown elsewhere (Ostrovsky and Argon, unpublished data), GRP94 interacts physically with IGF-II, and this interaction may explain the previous observations that GRP94 expression is important to maintain fusion competence (Gorza and Vitadello, 2000; Vitadello *et al.*, 2003).

IGF-II is known to be expressed in the early postimplantation rodent embryo (Heath and Shi, 1986; Beck *et al.*, 1987). IGF-II transcripts were detected first in primitive endoderm and then in extraembryonic mesoderm at the early primitive streak stage (Lee *et al.*, 1990). Labeling in the embryo proper appears first at the late primitive streak/neural plate stage in lateral mesoderm and in anterior-proximal cells located between the visceral endoderm and the most cranial region of the embryonic ectoderm (Lee *et al.*, 1990). When IGF-II expression was ablated genetically, mesoderm development was impaired (Morali *et al.*, 2000). In both mouse and chicken embryogenesis, IGF-I is expressed at later stages than IGF-II (Baker *et al.*, 1993; Scanes *et al.*, 1997). Thus, IGF-II and IGF1R are a relevant ligand-receptor pair for cell fate decisions during mesoderm induction, and if IGF secretion is dependent on GRP94, the observed phenotype is consistent with published work.

The genetic inference that GRP94 activity is necessary for the maturation and secretion of active IGF hormones is supported by biochemical data. The ability of several cell lines to withstand serum withdrawal depends on their capacity to secrete IGF-I or IGF-II, which in turn is regulated by GRP94, and this regulation is mediated by physical association of GRP94 with intracellular proIGF (Ostrovsky and Argon, unpublished data). One possible prediction is that the intracellular level or distribution of IGF-II in embryonic cells that express this growth factor will be different in *grp94−/−* embryos. However, tests of this prediction have so far proven inconclusive, due to the quality of the available antibody.

It is likely that GRP94 has functions other than control of IGF-II in early mouse development and in muscle differentiation: although *grp94−/−* embryos invariably die in utero, targeted deletion of IGF-II, IGF-I, or IGF-I receptor does not cause early embryonic lethality as does the ablation of *grp94* (DeChiara *et al.*, 1990; Baker *et al.*, 1993; Liu *et al.*, 1993). Thus, we surmise that GRP94's activity is needed for additional developmentally relevant client(s). It is possible that one client is an integrin, as Randow and Seed (2001) showed selective dependence of cell surface expression of some integrins on GRP94. Other potential GRP94 client proteins in early development are the Toll-like receptors 1, 2, and 4. Toll was originally identified in *Drosophila* embryos (Anderson *et al.*, 1985) and then in *Xenopus* embryos (Prothmann *et al.*, 2000) as critically important for axis formation. However, in higher eukaryotes, multiple Toll-like receptors are present and although some are clients of GRP94 (Randow and Seed, 2001), none has so far been shown definitively to function in early mammalian development.

A number of other secreted and membrane-bound proteins have been shown by genetic ablation to be important at the time of primitive streak formation and gastrulation. These include fibroblast growth factor receptors, activin receptors, bone morphogenetic receptors, and several of their respective ligands (Roelen *et al.*, 1997; Gu *et al.*, 1998; Weinstein *et al.*, 1998; Mishina *et al.*, 1999). It is not known if any of these proteins depend on GRP94 for membrane expression or secretion, but all are potential clients due to the requirement to pass the ER quality control before they are either secreted or deposited on the plasma membrane.

In summary, this work shows that IGF-II production in early mouse embryos depends critically on the activity of the chaperone GRP94, and we hypothesize that other developmentally important proteins are similarly affected. In the absence of GRP94, these clients would not fold properly and would not be released by the ER quality control machinery for transport to the cell surface. This in turn would prevent critical ligand-receptor interactions from taking place, and intercellular interactions that are required for differentiation would be precluded.

Note added in proof. While this manuscript was in preparation, Yang *et al.* (2007) reported the generation of a conditional GRP94/gp96 knockout mouse and showed that this HSP is not critical for the proliferation and differentiation of macrophages in vivo.

ACKNOWLEDGMENTS

We thank Hong Luo for help in screening for correctly targeted ES clones and Huiping Liu for help in deriving ES cell lines from the mice, Dr. M. Green (St. Louis University) for the murine GRP94 cDNA clone pGEM99.2, Dr. P. Labosky (University of Pennsylvania) for plasmids and probes for in situ hybridization, Dr. R. C. Mulligan (Children's Hospital, Boston) for the targeting vector pPNT, Dr. B. Hendrickson (University of Chicago) for the C1 ES cell line, Dr. Baserga (Thomas Jefferson Medical School) for the p12 cells, and Dr. J. Golden and his lab (Children's Hospital, Philadelphia) for the use of the microscopy setup and their advice. This work was supported by grants from the National Institutes of Health (NIH), W. W. Smith Foundation, and the Pennsylvania Department of Health to Y.A. B.B.S. and T.G. were supported in part by NIH predoctoral training grants, S.W. by a fellowship from the American Cancer Society, and O.O. by a fellowship from the Juvenile Diabetes Research Foundation.

REFERENCES

Anderson, K. V., Bokla, L., and Nusslein-Volhard, C. (1985). Establishment of dorsal-ventral polarity in the *Drosophila* embryo: the induction of polarity by the Toll gene product. Cell *42*, 791–798.

Bain, G., Kitchens, D., Yao, M., Huettner, J. E., and Gottlieb, D. I. (1995). Embryonic stem cells express neuronal properties in vitro. Dev. Biol. *168*, 342–357.

Baker, J., Liu, J. P., Robertson, E. J., and Efstratiadis, A. (1993). Role of insulin-like growth factors in embryonic and postnatal growth. Cell *75*, 73–82.

Barnes, J. A., and Smoak, I. W. (1997). Immunolocalization and heart levels of GRP94 in the mouse during post-implantation development. Anat. Embryol. *196*, 335–341.

Barnes, J. D., Crosby, J. L., Jones, C. M., Wright, C. V., and Hogan, B. L. (1994). Embryonic expression of Lim-1, the mouse homolog of *Xenopus* Xlim-1, suggests a role in lateral mesoderm differentiation and neurogenesis. Dev. Biol. *161*, 168–178.

Beck, F., Samani, N. J., Penschow, J. D., Thorley, B., Tregear, G. W., and Coghlan, J. P. (1987). Histochemical localization of IGF-I and -II mRNA in the developing rat embryo. Development *101*, 175–184.

Boheler, K. R., Czyz, J., Tweedie, D., Yang, H. T., Anisimov, S. V., and Wobus, A. M. (2002). Differentiation of pluripotent embryonic stem cells into cardiomyocytes. Circ. Res. *91*, 189–201.

Ciruna, B. G., and Rossant, J. (1999). Expression of the T-box gene Eomesodermin during early mouse development. Mech. Dev. *81*, 199–203.

Coucouvanis, E., and Martin, G. R. (1999). BMP signaling plays a role in visceral endoderm differentiation and cavitation in the early mouse embryo. Development *126*, 535–546.

Dani, C., Smith, A. G., Dessolin, S., Leroy, P., Staccini, L., Villageois, P., Darimont, C., and Ailhaud, G. (1997). Differentiation of embryonic stem cells into adipocytes in vitro. J. Cell Sci. *110*, 1279–1285.

Dechert, U., Weber, P., Konig, B., Ortwein, C., Nilson, I., Linxweiler, W., Wollny, E., and Gassen, H. G. (1994). A protein kinase isolated from porcine brain microvessels is similar to a class of heat-shock proteins. Eur. J. Biochem. *225*, 805–809.

DeChiara, T. M., Efstratiadis, A., and Robertson, E. J. (1990). A growth-deficiency phenotype in heterozygous mice carrying an insulin-like growth factor II gene disrupted by targeting. Nature *345*, 78–80.

Drummond, I. A., Lee, A. S., Resendez, E., Jr., and Steinhardt, R. A. (1987). Depletion of intracellular calcium stores by calcium ionophore A23187 induces the genes for glucose-regulated proteins in hamster fibroblasts. J. Biol. Chem. *262*, 12801–12805.

Dufort, D., Schwartz, L., Harpal, K., and Rossant, J. (1998). The transcription factor HNF3beta is required in visceral endoderm for normal primitive streak morphogenesis. Development *125*, 3015–3025.

Duguay, S. J., Jin, Y., Stein, J., Duguay, A. N., Gardner, P., and Steiner, D. F. (1998). Post-translational processing of the insulin-like growth factor-2 precursor. Analysis of O-glycosylation and endoproteolysis. J. Biol. Chem. *273*, 18443–18451.

Duncan, S. A., Nagy, A., and Chan, W. (1997). Murine gastrulation requires HNF-4 regulated gene expression in the visceral endoderm: tetraploid rescue of Hnf-4(−/−) embryos. Development *124*, 279–287.

Dupont, J., and Holzenberger, M. (2003). Biology of insulin-like growth factors in development. Birth Defects Res. Part C Embryo Today *69*, 257–271.

Gass, J. N., Gifford, N. M., and Brewer, J. W. (2002). Activation of an unfolded protein response during differentiation of antibody-secreting B cells. J. Biol. Chem. *277*, 49047–49054.

Gorza, L., and Vitadello, M. (2000). Reduced amount of the glucose-regulated protein GRP94 in skeletal myoblasts results in loss of fusion competence. FASEB J. *14*, 461–475.

Gu, Z., Nomura, M., Simpson, B. B., Lei, H., Feijen, A., van den Eijnden-van Raaij, J., Donahoe, P. K., and Li, E. (1998). The type I activin receptor ActRIB is required for egg cylinder organization and gastrulation in the mouse. Genes Dev. *12*, 844–857.

Guo, L., Nakamura, K., Lynch, J., Opas, M., Olson, E. N., Agellon, L. B., and Michalak, M. (2002). Cardiac-specific expression of calcineurin reverses embryonic lethality in calreticulin-deficient mouse. J. Biol. Chem. *277*, 50776–50779.

Heath, J. K., and Shi, W. K. (1986). Developmentally regulated expression of insulin-like growth factors by differentiated murine teratocarcinomas and extraembryonic mesoderm. J. Embryol. Exp. Morphol. *95*, 193–212.

Hogan, B. L., Beddington, R. S., Constantini, F., and Lacy, E. (1994). Manipulating the Mouse Embryo, a Laboratory Manual, 2nd ed., Cold Spring Harbor, NY: Cold Spring Harbor Laboratory Press.

Ishiguro, S., Watanabe, Y., Ito, N., Nonaka, H., Takeda, N., Sakai, T., Kanaya, H., and Okada, K. (2002). SHEPHERD is the *Arabidopsis* GRP94 responsible for the formation of functional CLAVATA proteins. EMBO J. *21*, 898–908.

Kim, S. K., Kim, Y. K., and Lee, A. S. (1990). Expression of the glucose-regulated proteins (GRP94 and GRP78) in differentiated and undifferentiated mouse embryonic cells and the use of the GRP78 promoter as an expression system in embryonic cells. Differentiation *42*, 153–159.

Kim, Y. K., Kim, K. S., and Lee, A. S. (1987). Regulation of the glucose-regulated protein genes by β-mercaptoethanol requires de novo protein synthesis and correlates with inhibition of protein glycosylation. J. Cell. Physiol. *133*, 553–559.

Lammert, E., Arnold, D., Rammensee, H. G., and Schild, H. (1996). Expression levels of stress protein gp96 are not limiting for major histocompatibility complex class I-restricted antigen presentation. Eur. J. Immunol. *26*, 875–879.

Lee, A. S., Delegeane, A. M., Baker, V., and Chow, P. C. (1983). Transcriptional regulation of two genes specifically induced by glucose starvation in a hamster mutant fibroblast cell line. J. Biol. Chem. *258*, 597–603.

Lee, J. E., Pintar, J., and Efstratiadis, A. (1990). Pattern of the insulin-like growth factor II gene expression during early mouse embryogenesis. Development *110*, 151–159.

LeRoith, D., and Roberts, C. T., Jr. (2003). The insulin-like growth factor system and cancer. Cancer Lett. *195*, 127–137.

Lewis, M. J., Mazzarella, R. A., and Green, M. (1985). Structure and assembly of the endoplasmic reticulum. The synthesis of three major endoplasmic reticulum proteins during lipopolysaccharide-induced differentiation of murine lymphocytes. J. Biol. Chem. *260*, 3050–3057.

Li, L. J., Li, X., Ferrario, A., Rucker, N., Liu, E. S., Wong, S., Gomer, C. J., and Lee, A. S. (1992). Establishment of a Chinese hamster ovary cell line that expresses grp78 antisense transcripts and suppresses A23187 induction of both GRP78 and GRP94. J. Cell. Physiol. *153*, 575–582.

Li, X. A., and Lee, A. S. (1991). Competitive inhibition of a set of endoplasmic reticulum protein genes (GRP78, GRP94, and ERp72) retards cell growth and lowers viability after ionophore treatment. Mol. Cell. Biol. *11*, 3446–3453.

Little, E., and Lee, A. S. (1995). Generation of a mammalian cell line deficient in glucose-regulated protein stress induction through targeted ribozyme driven by a stress- inducible promoter. J. Biol. Chem. *270*, 9526–9534.

Liu, J. P., Baker, J., Perkins, A. S., Robertson, E. J., and Efstratiadis, A. (1993). Mice carrying null mutations of the genes encoding insulin-like growth factor I (Igf-1) and type 1 IGF receptor (Igf1r). Cell *75*, 59–72.

Maki, R. G., Eddy, R. L., Jr., Byers, M., Shows, T. B., and Srivastava, P. K. (1993). Mapping of the genes for human endoplasmic reticular heat shock protein gp96/grp94. Somat. Cell Mol. Genet. *19*, 73–81.

McCormick, P. J., and Babiarz, B. (1984). Expression of a glucose-regulated cell surface protein in early mouse embryos. Dev. Biol. *105*, 530–534.

Melnick, J., Dul, J. L., and Argon, Y. (1994). Sequential interaction of the chaperones BiP and GRP94 with immunoglobulin chains in the endoplasmic reticulum. Nature *370*, 373–375.

Mishina, Y., Crombie, R., Bradley, A., and Behringer, R. R. (1999). Multiple roles for activin-like kinase-2 signaling during mouse embryogenesis. Dev. Biol. *213*, 314–326.

Morali, O. G., Jouneau, A., McLaughlin, K. J., Thiery, J. P., and Larue, L. (2000). IGF-II promotes mesoderm formation. Dev. Biol. *227*, 133–145.

Myer, A., Olson, E. N., and Klein, W. H. (2001). MyoD cannot compensate for the absence of myogenin during skeletal muscle differentiation in murine embryonic stem cells. Dev. Biol. *229*, 340–350.

Palmieri, S. L., Peter, W., Hess, H., and Scholer, H. R. (1994). Oct-4 transcription factor is differentially expressed in the mouse embryo during establishment of the first two extraembryonic cell lineages involved in implantation. Dev. Biol. *166*, 259–267.

Prothmann, C., Armstrong, N. J., and Rupp, R. A. (2000). The Toll/IL-1 receptor binding protein MyD88 is required for *Xenopus* axis formation. Mech. Dev. *97*, 85–92.

Randow, F., and Seed, B. (2001). Endoplasmic reticulum chaperone gp96 is required for innate immunity but not cell viability. Nat. Cell Biol. *3*, 891–896.

Robert, J., Menoret, A., Basu, S., Cohen, N., and Srivastava, P. R. (2001). Phylogenetic conservation of the molecular and immunological properties of the chaperones gp96 and hsp70. Eur. J. Immunol. *31*, 186–195.

Roelen, B. A., Goumans, M. J., van Rooijen, M. A., and Mummery, C. L. (1997). Differential expression of BMP receptors in early mouse development. Int. J. Dev. Biol. *41*, 541–549.

Rosser, M.F.N., and Nicchitta, C. V. (2000). Ligand interactions in the adenosine nucleotide binding domain of the Hsp90 chaperone, GRP94. I. Evidence for allosteric regulation of ligand binding. J. Biol. Chem. *275*, 22798–22805.

Russ, A. P. *et al.* (2000). Eomesodermin is required for mouse trophoblast development and mesoderm formation. Nature *404*, 95–99.

Scanes, C. G., Thommes, R. C., Radecki, S. V., Buonomo, F. C., and Woods, J. E. (1997). Ontogenic changes in the circulating concentrations of insulin-like growth factor (IGF)-I, IGF-II, and IGF-binding proteins in the chicken embryo. Gen. Comp. Endocrinol. *106*, 265–270.

Schulte, T. W. *et al.* (1999). Interaction of radicicol with members of the heat shock protein 90 family of molecular chaperones. Mol. Endocrinol. *13*, 1435–1448.

Simeone, A., Acampora, D., Mallamaci, A., Stornaiuolo, A., D'Apice, M. R., Nigro, V., and Boncinelli, E. (1993). A vertebrate gene related to orthodenticle contains a homeodomain of the bicoid class and demarcates anterior neuroectoderm in the gastrulating mouse embryo. EMBO J. *12*, 2735–2747.

Srivastava, P. K., Kozak, C. A., and Old, L. J. (1988). Chromosomal assignment of the gene encoding the mouse tumor rejection antigen gp96. Immunogenetics *28*, 205–207.

Thomas, P. Q., Brown, A., and Beddington, R. S. (1998). Hex: a homeobox gene revealing peri-implantation asymmetry in the mouse embryo and an early transient marker of endothelial cell precursors. Development *125*, 85–94.

Tybulewicz, V. L., Crawford, C. E., Jackson, P. K., Bronson, R. T., and Mulligan, R. C. (1991). Neonatal lethality and lymphopenia in mice with a homozygous disruption of the c-abl proto-oncogene. Cell *65*, 1153–1163.

Varlet, I., Collignon, J., and Robertson, E. J. (1997). nodal expression in the primitive endoderm is required for specification of the anterior axis during mouse gastrulation. Development *124*, 1033–1044.

Vitadello, M., Penzo, D., Petronilli, V., Michieli, G., Gomirato, S., Menabo, R., Di Lisa, F., and Gorza, L. (2003). Overexpression of the stress protein Grp94 reduces cardiomyocyte necrosis due to calcium overload and simulated ischemia. FASEB J. *17*, 923–925.

Vogen, S. M., Gidalevitz, T., Biswas, C., Simen, B. S., Stein, E., Gulmen, F., and Argon, Y. (2002). Radicicol-sensitive peptide binding to the N-terminal portion of GRP94. J. Biol. Chem. *277*, 40742–40750.

Voss, A. K., Thomas, T., and Gruss, P. (2000). Mice lacking HSP90beta fail to develop a placental labyrinth. Development *127*, 1–11.

Weinstein, M., Yang, X., Li, C., Xu, X., Gotay, J., and Deng, C. X. (1998). Failure of egg cylinder elongation and mesoderm induction in mouse embryos lacking the tumor suppressor smad2. Proc. Natl. Acad. Sci. USA *95*, 9378–9383.

Wiest, D. L., Burkhardt, J. K., Hester, S., Hortsch, M., Meyer, D. I., and Argon, Y. (1990). Membrane biogenesis during B cell differentiation: most endoplasmic reticulum proteins are expressed coordinately. J. Cell Biol. *110*, 1501–1511.

Wilkinson, D. G., Bhatt, S., and Herrmann, B. G. (1990). Expression pattern of the mouse T gene and its role in mesoderm formation. Nature *343*, 657–659.

Yaffe, D., and Saxel, O. (1977). Serial passaging and differentiation of myogenic cells isolated from dystrophic mouse muscle. Nature *270*, 725–727.

Yamada, T., Yoshikawa, M., Kanda, S., Kato, Y., Nakajima, Y., Ishizaka, S., and Tsunoda, Y. (2002). In vitro differentiation of embryonic stem cells into hepatocyte-like cells identified by cellular uptake of indocyanine green. Stem Cells *20*, 146–154.

Yang, Y., Liu, B., Dai, J., Srivastava, P. K., Zammit D. J., Lefrançois, L., and Li, Z. (2007). Heat shock protein gp96 is a master chaperone for toll-like receptors and is important in the innate function of macrophages. Immunity *26*, 215–226.

Yoon, J. K., Moon, R. T., and Wold, B. (2000). The bHLH class protein pMesogenin1 can specify paraxial mesoderm phenotypes. Dev. Biol. *222*, 376–391.